Macromolecular Research, Vol. 11, No. 6, pp 410-417 (2003)

Synthesis and Properties of Exfoliated Poly(methyl methacrylate-*co*-acrylonitrile)/Clay Nanocomposites via Emulsion Polymerization

Mingzhe Xu, Yeong Suk Choi, Ki Hyun Wang, Jong Hyun Kim, and In Jae Chung*

Department of Chemical and Biomolecular Engineering, Korea Advanced Institute of Science and Technology (KAIST), 373-1, Guseong-dong, Yuseong-gu, Daejeon 305-701, Korea

Received Oct. 5, 2002; Revised Sept. 16, 2003

Abstract: Poly(methyl methacrylate-*co*-acrylonitrile) [P(MMA-*co*-AN)]/Na-MMT nanocomposites were synthesized through emulsion polymerization with pristine Na-MMT. The nanocomposites were exfoliated up to 20 wt% content of pristine Na-MMT relative to the amount of MMA and AN, and exhibited enhanced storage moduli, E', relative to the neat copolymer. The exfoliated morphology of the nanocomposite was confirmed by XRD and TEM. 2-Acrylamido-2-methyl-1-propane sulfonic acid (AMPS) widened the galleries between the clay layers before polymerization and facilitated the comonomers, penetration into the clay to create the exfoliated nanocomposites. The onset of the thermal decomposition of the nanocomposites shifted to a higher temperature as the clay content increased. By calculating areas of tanδ of the nanocomposites, we observed that the nanocomposites show more solid-like behavior as the clay content increases. The dynamic storage modulus and complex viscosity increased with clay content. The complex viscosity showed shear-thinning behavior as the clay content increased. The Young's moduli of the nanocomposites are higher than that of the neat copolymer and they increase steadily as the silicate content increases, as a result of the exfoliated structure at high clay content.

Keywords: PMMA, AN, emulsion, clay, nanocomposite, Na-MMT, AMPS.

Introduction

Polymer/silicate nanocomposites are a novel class of composite exhibiting enhanced mechanical,[1] thermal,[2] and barrier properties[3] by adding just a small fraction of clay to a polymer matrix. Pioneering work of polymer-clay nanocomposites was done by researchers at Toyota for light weight materials applications.[4] The potential property enhancements have led to the application in various fields such as packaging, electronics, automobile industry and etc.

Generally there are two types of nanostructure; Intercalated and exfoliated nanostructures. When polymer chains are inserted between the silicate layers resulting in a well ordered multiplayer structure built up with alternating polymeric and inorganic layers, intercalated structures are obtained. Exfoliated structures are needed for the improved mechanical and thermal properties because of homogeneous dispersion of clay and large interfacial area of clay layers.

Many researchers have reported the fabrication of polymer/clay nanocomposites.[5-23] Copolymer of acrylonitrile and methyl methacrylate are widely used as fibers to make knitted clothing, like socks and sweaters, as well as outdoor products like tents. But the research on polymer/silicate nanocomposite with copolymers of methyl acrylate and acrylonitrile has been rare. So, it is desirable to synthesize and study copolymer/Na-MMT of methyl acrylate and acrylonitrile industrially.

To make an exfoliated polymer/clay nanocomposite, it is very important to let clay layers disperse homogeneously in polymer matrix. But it is difficult to obtain idealized exfoliated morphology because of hydrophilicity of pristine clay in hydrophobic polymer matrix. Usually the clay is modified with alkylammonium for two purposes. One is to widen the gallery of the layered silicate and to make polymer penetrate easily into clay layer space. Second is to get alkylammonium molecules tethered on silicate surface and make silicate layers miscible with hydrophobic polymer.

In our recent article on the fabrication of polymer/clay nanocomposite through emulsion polymerization we used water to make the basal space of silicate layers widen without any chemical treatment.[24,25] We will extend this method to copolymerization of MMA and AN and describe a simple and convenient way to obtain exfoliated P(MMA-*co*-AN)/Na-MMT nanocomposites through in-situ polymerization with 2-acrylamido-2-methyl-1-propane sulfonic acid (AMPS)[26]

*e-mail: chung@kaist.ac.kr
1598-5032/12/410-08

in presence of pristine Na-MMT.

In this paper, we show that MMA and AN penetrated into the layers of clay, enlarging the basal spacing of clay layers before polymerization. Furthermore, AMPS made further enlarge the basal space of the clay dispersion. It is believed that MMA and AN would polymerize within and near silicate layers. This behavior may be contributed to the exfoliation of clay layers in nanocomposites.

The P(MMA-*co*-AN)/Na-MMT nanocomposites were synthesized and characterized by a simple and convenient emulsion polymerization with a reactive surfactant AMPS. In addition, we investigated their mechanical, thermal, and rheological properties.

Experimental

Materials. The clay used is sodium montmorillonite (Na-MMT) from Kunimine Co. and It has a cation exchange capacity (CEC) of 119 meq/100 g.

Acrylonitrile (AN), methylmethacrylate, 2-acrylamido-2-methyl-1-propane sulfonic acid (AMPS), and dodecylbenzenesulfonic acid sodium salt (DBS-Na) were purchased from Aldrich and used without further purificaton. Pristine Na-MMT was dispersed in deionized water for 24 hrs at ambient temperature before polymerization. Potassium persulate (KPS) from Junsei, an initiator, was recrystallized using a deionized water. *N,N*-Dimethylformamide (DMF), HPLC solvent grade, was purchased from Aldrich for polymer recovery in the reverse ion exchange. Methyl alcohol (MeOH) of Fluka, a non-solvent for P(MMA-*co*-AN), was distilled at normal pressure. Lithium chloride (Junsei) was recrystallized with THF.

Fabricaton of P(MMA-*co*-AN)/Na-MMT Nanocomposites. Polymerization was Carried out in Two Stages:

1. Pristine Na-MMT dispersed in deionized water(from 0 to 20 wt% of Na-MMT relative to weight of comonomer) with 10 g of mixture of monomers (MMA/AN = 5 g/5 g) and 0.6 g of AMPS, and the mixture were stirred at room temperature in a 1 L four-neck round bottom flask. The flask was equipped with a baffle stirrer, a reflux condenser, a nitrogen inlet, and a rubber septum. 40 g of initiator solution (KPS/water ratio = 1 g/99 g) was injected into the flask through a rubber septum by using a glass syringe. The mixture was stirred at 200 rpm for 1 hr under nitrogen atmosphere at room temperature. Initial polymerization was performed at 65 °C for 1 hr. In the presence of Na-MMT, white particles were generated within 10 min after the initiator injection. Then 10 g of DBS-Na aqueous solution was added to stabilize the particle in order to obtain a high conversion of polymerization. After adding DBS-Na we control reaction process directly to second stage.

2. After the initial polymerization was completed, 30 g of mixture of monomers (MMA/AN = 20 g/20 g) was fed at the rate of 0.32 cc/min into the flask through a septum by using a syringe pump. After monomer feeding was completed, additional 10 g of KPS was added. Continuously the mixture was stirred for additional 4 hrs for polymerization after temperature was raised up to 85 °C. The sample was recovered from the flask and dried with a freeze-drying equipment for 6 days and further dried in a high vacuum oven at 80 °C for 3 days.

The nanocomposite was marked by the letters A, N, M and T followed by a number. The letter A, M, N and T denote AMPS, methyl methacrylate (MMA), acrylonitrile (AN), and clay (Na-MMT) respectively. The number followed by M and N stands for weight of each monomer used in emulsion polymerization and the number following after T stands for weight percent of clay relative to monomers. For example, A0.6M20N20T5 nanocomposite includes 0.6 g of AMPS, 20 g of MMA, 20 g of AN, 5 wt% Na-MMT relative to 40 g of comonomer (MMA and AN).

Before X-ray measurements a small amount of nanocomposites was extracted with hot THF in a Soxhlet extractor for 12 hrs at 110 °C to remove oligomers, water molecules, or surfactants. Because small molecules may expand the interlayer space of Na-MMT, as if the polymers exfoliate the layers. These extracted polymer/Na-MMT nanocomposites were dried under a highly reduced pressure at 80 °C for 50 hrs and molded in a disc type at a nominal 3,000 psi of pressure. Their basal spaces were calculated from X-ray patterns using Bragg equation.

Polymer Recovery. Polymers in the nanocomposites were totally recovered by reverse ion exchange procedure decribed in the following way: 1 g of a prepared nanocomposite, 0.3 g of LiCl[27] and 80 mL of DMF were stirred under a nitrogen atmosphere at 80 °C for 5 days in a 500 mL three-neck reactor fitted with a condenser, a nitrogen inlet, and an outlet. The suspension was centrifuged at 6,000 rpm for 30 min to separate polymers from the silicate cakes. After separating the clay by centrifugation, the polymeric material was recovered by precipitation in MeOH(10-20 fold) with 0.45 μm membrane filter and then dried in the same way as the THF extraction. These copolymers were supplied to measure molecular weight by GPC.

Characterization. Fourier transform infrared spectroscopy (FT-IR) was performed on a infrared spectrometer(Bomem 102 model) at 4 cm^{-1} resolution. Infrared spectrum on KBr pellets was averaged over 20 scans on a FT-IR spectrometer.

Wide-angle X-ray diffraction (WAXD) analysis was performed on a Rigaku X-ray generator (CuKα Radiation with λ = 0.15406 nm) at a room temperature. A sample was prepared in the pellet form. The diffractograms were scanned at the rate of 2°/min in 2θ range of 1.2-10°. The basal spaces of pristine Na-MMT in the solution of AMPS, comonomer and water were measured by powder X-ray diffraction method (using powder holder to hold the solution state sample).

Molecular weight analysis was performed at room temperature by gel permeation chromatography (GPC). Water

GPC system equipped with six styragel HR columns (two 500, two10^3, 10^4,and 10^5) and Water 410 RID detector was used with the flow rate of THF 2.0 mL/min after calibration with 10 PS standards.

Thermogravimetric analysis (TGA) was performed on a thermogravimetric analyzer (TA instruments) with a Perkin-Elmer thermobalance over the temperature range 25-600 °C at the scan rate of 10 °C/min under nitrogen atmosphere. The microstructure of nanocomposite was imaged using a transmission electron microscopy (TEM), Phillips CM-20. Acceleration voltage of TEM was 160 kV. The nanocomposite was sectioned into ultrathin slices (< 100 nm) using microtome equipped with a diamond knife at a room temperature. Dynamic mechanical properties of nanocomposites were measured using a Rheometric Scientific DMTA4 with extensional mode. Dynamic moduli and tanδ of all samples were measured at the scan rate of 4 °C/min from 30 to 180 °C under 0.01% deformation at a frequency of 1Hz. The bar type specimens were molded at 175 °C with dimensions 40 × 10× 0.75 mm thick using a hot press.

Rheology measurements of nanocomposites were performed on an Advanced Rheometric Expansion System (ARES) in oscillatory mode with a parallel plate geometry using 25 mm diameter plates at 200 °C. Samples for melt rheology were molded in disk shapes by compression. Typical sample thickness had the range from 1.0 to 1.2 mm. For the linear viscoelastic measurements dynamic test was firstly performed for 1hr (at frequency = 10 Hz, strain = 0.01%, which is well in the linear dynamic region) at 200 °C. All the experiments were performed under a nitrogen atmosphere to minimize oxidative degradation of specimens.

Tensile test specimens were prepared by molding in a dumb-bell shaped molder on a hot press at 165 °C for 2 min. Tensile tests were performed at room temperature on Instron tester (model 8032) according to ASTM 638-94. The samples were deformed with a 1 mm/min extension rate. The tests were carried out at 20 °C and 70% relative humidity. At least, five specimens were tested for each set of samples and the mean values were reported.

Results and Discussion

Molecuar weights of P(MMA-*co*-AN) obtained by the extraction of nanocomposite with DMF are listed in Table I. The M_w values of the copolymers are found to be in the order of 10^5 g/mol, regardless the silicate content. It is believed that molecular weights is not affected by the amount of clay in the range of conventional surfactant content used in our system.

Figure 1 shows the FT-IR spectra of Na-MMT, AMPS, neat copolymer, and A0.3M20N20T10. The sharp peak at 1043 cm^{-1} is associated with the Si-O stretching vibration of silicate layer, and peaks at about 600 and 410 cm^{-1} were assigned to the stretching of Al-O and bending of Si-O in Na-MMT. The peaks at 1610 cm^{-1} (vinyl stretching), 1364-1241 cm^{-1} (S=O), N-H bending 1543 cm^{-1} are related to AMPS. Absorption bands at 2953 cm^{-1} (C-H stretching), 1730 cm^{-1} (C=O stretching), 1219 and 1143 cm^{-1} (C-O stretching), 1043 cm^{-1} (neighboring Si-O stretching), 2240 cm^{-1} (C≡N stretching), and 1456 cm^{-1} (C-H bending) are the consequences of the P(MMA-*co*-AN)/copolymer. Disappearance of the absorbance peak at 1610 cm^{-1} corresponding to vinyl stretching of AMPS reveals the high conversion of monomers in the polymerization for the nanocomposites fabrication.

The pristine Na-MMT has an interlayer *d*-spacing of 1.14 nm with 2θ value 7.7°, which is obtained from the peak

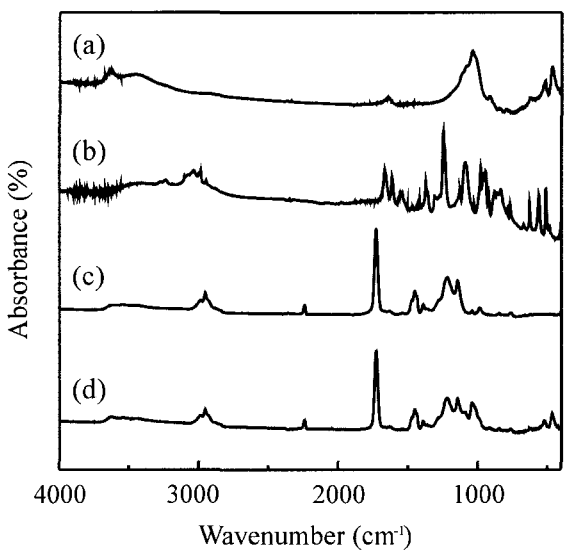

Figure 1. FT-IR spectra of (a) pristine Na-MMT, (b) AMPS (reactive surfactant), (c) A0.6M20N20T0 (neat copolymer), and (d) A0.6M20N20T10 nanocomposite (containing 10 wt% of Na-MMT).

Table I. Molecular Weights of Polymeric Materials Recovered from P(MMA-*co*-AN)/Na-MMT Nanocomposite Series and Neat Copolymer Prepared

Sample Code	$M_n \times 10^4$ (g/mol)	$M_w \times 10^5$ (g/mol)	PDI (M_w/M_n)
A0.6N20M20T0	15.78	54.39	3.45
A0.6N20M20T5	24.89	69.95	2.81
A0.6N20M20T10	18.52	59.80	3.23
A0.6N20M20T20	18.40	62.88	3.42

position (d_{001}-reflection) of WAXD traces by using Bragg equation: $2d_{001}\sin\theta = \lambda$

where d_{001} is the interplanar distance of (001) reflection plane, θ is the diffraction angle and λ is the wavelength.

The XRD patterns of pristine Na-MMT dispersed in various solution conditions are shown in Figure 2 before polymerization. The peak of Na-MMT dispersed in water is occurred at 5.7° corresponding to the basal space of 1.55 nm, which means the interlayer space of silicate is widened by the presence of water. The Na-MMT dispersed with comonomer in water shows broad peak around 4.5~5.7° with the d_{001} space of about 1.96~1.55 nm. The Na-MMT dispersed with AMPS in water shows the peak around 3.5° with the space of 2.52 nm. The Na-MMT dispersion with AMPS and comonomer in water shows no peak. It indicates that AMPS intercalated in clay attracts comonomer to make the clay layers exfoliated.

Figure 3 shows a series of thin film XRD patterns obtained from pristine Na-MMT and nanocomposites extracted by using a Soxhlet extration apparatus with THF. Diffraction patterns of all A0.6M20N20T nanocomposite series prepared show no peaks, indicating that Na-MMT is exfoliated in polymer matrix up to 20 wt% of silicates.

The complete exfoliation of the silicate layers cannot be judged from only these diffractograms. Transmission electron microscopy (TEM) was adopted to confirm the morphology of the extracted nanocomposite. Figure 4 shows TEM micrograph of extracted A0.6M20N20T10 nanocomposite which is exfoliated as revealed by XRD. The dark lines in the figure correspond to the silicate layers. Micron-sized clay tactoids do not exist in the nanocomposite. The clay layers are well exfoliated in the polymer matrix and large silicate particles are absent.

The TGA analysis of nanocomposites is shown in Figure 5. The onset temperature of thermal decomposition moves toward a higher temperature as the clay content increases. All the exfoliated nanocomposites show elevated onset of thermal decomposition relative to pure copolymer. The pure copolymer starts to decompose at about 270°C, but the

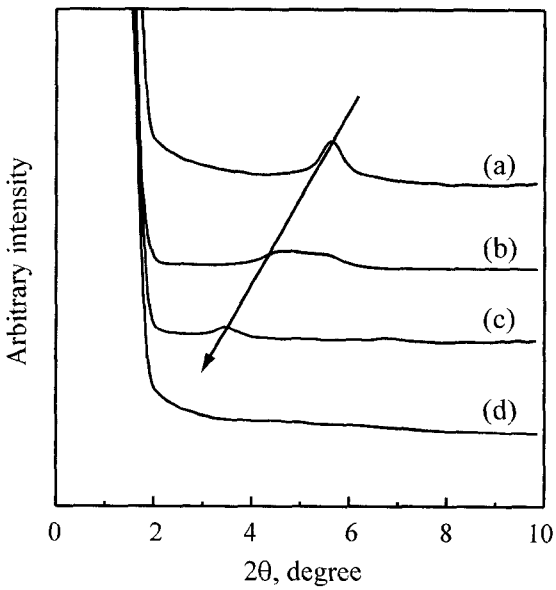

Figure 2. X-ray diffraction patterns of water dispersions of pristine Na-MMT under various conditions: (a) the dispersion of Na-MMT in water, (b) with AMPS, and (c) with comonomer, and (d) with both AMPS and comonomer.

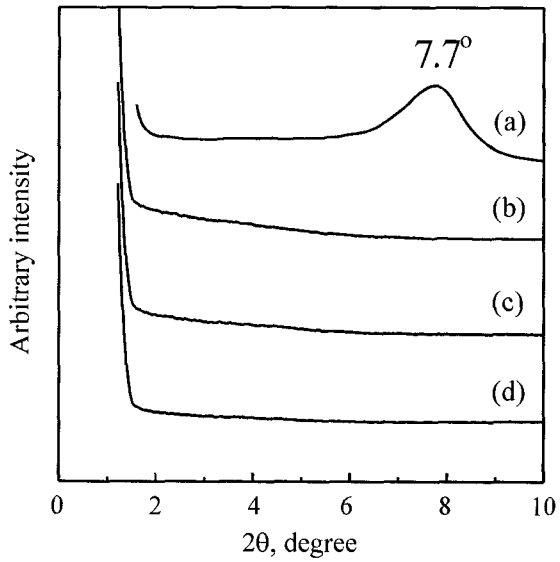

Figure 3. X-ray diffraction patterns of pristine Na-MMT and extracted M20N20T nanocomposite series with THF. (a) pristine Na-MMT, (b) A0.6M20N20T20, (c) A0.6M20N20T10, and (d) A0.6M20N20T5.

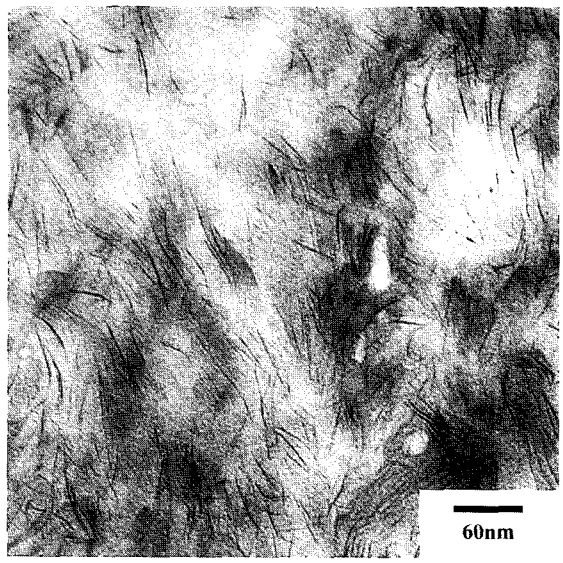

Figure 4. Transmission electron microscopy (TEM) image of extracted A0.6M20N20T10 nanocomposite.

nanocomposites are thermally stable up to 350 °C. The decomposition temperature of neat copolymer at 20% weight loss is 354 °C. A0.6M20N20T20 nanocomposite shows 13.7 °C increase in decomposition temperature at 20% weight loss relative to neat copolymer. This may result from the clay platelets in polymer matrix. In temperature range of more than 500 °C, a considerable amount of residue in the sample is observed, reaching a weight percentage of 20-40%.

Figure 6 illustrates the trend of storage modulus, E', as a function of the temperature for nanocomposites. The storage modulus of a nanocomposite increases with the amount of silicate. At 40 °C, A0.6M20N20T5 shows a 30%, A0.6M20N20T10 a 100%, and A0.6M20N20T20 a 163% increment of storage modulus relative to neat P(MMA-*co*-AN). Such large increment is due to homogeneous dispersion of exfoliated silicate layers in polymer matrix and high stiffness of individual sheet of MMT.

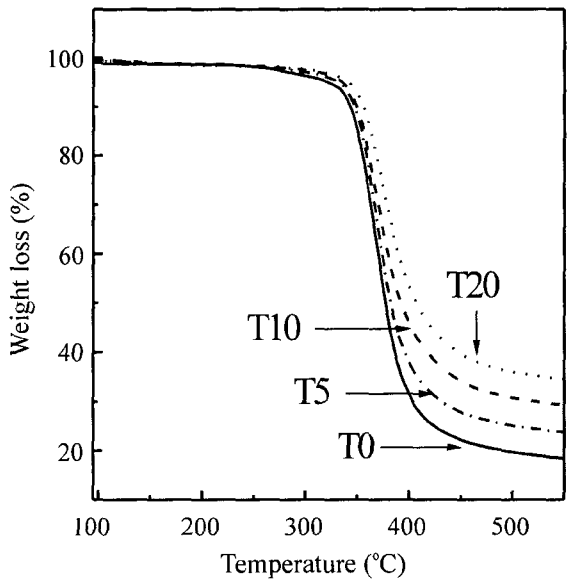

Figure 5. Thermal gravimetric curves for A0.6M20N20T nanocomposite series and neat copolymer under nitrogen atmosphere.

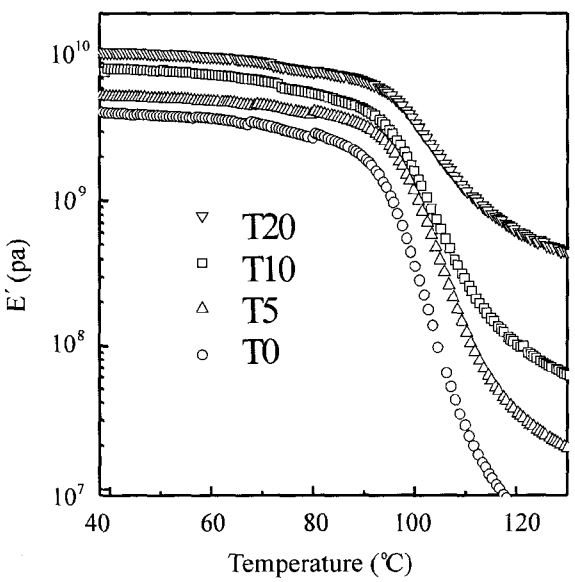

Figure 6. Dynamic storage moduli of unextracted A0.6M20N20T nanocomposite series as a function of temperature.

Figure 7 shows the temperature dependence of tanδ of the A0.6M20N20T nanocomposite series. The glass transition temperatures (T_g) were determined from center of peaks in the tanδ curves. The glass transition temperature of nanocomposites increase slightly as clay content increase and then decrease slightly at high clay loading in Table II.

It is not sufficient to consider T_g of DMTA as maximum temperature of nanocomposites. So the mechanical properties of nanocomposites are explained by regarding the ratio of viscous and elastic term additionally.

The equation of integration and the difference between unrelaxed modulus and relaxed modulus will be derived.

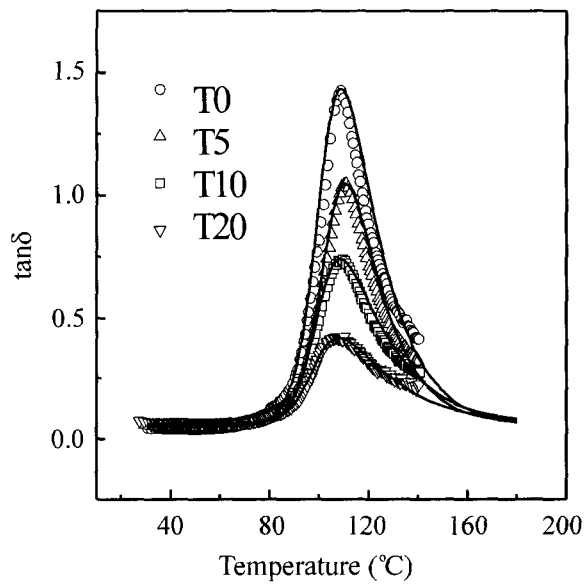

Figure 7. Tanδ of A0.6M20N20T nanocomposite series and neat copolymer as a function of temperature. The solid lines are fitted curves.

Table II. Tanδ Value of Nanocomposite and Peak Area of Tanδ Calculated from Fitted Curve

Sample Code	T_g (Tan δ)	Peak Area of Tanδ Calculated from Fitted Curve
A0.6N20M20T0%	108.83	46.2
A0.6N20M20T5%	111.04	31.73
A0.6N20M20T10%	109.82	24.99
A0.6N20M20T20%	106.99	14.44

$$\tan\delta = \frac{G''(\omega)}{G'(\omega)} = \frac{(G_u - G_r)\omega\tau}{G_r + \omega^2\tau^2 G_u} \quad (1)^{28}$$

where G', G'', G_u, G_r and τ are storage modulus, loss modulus, unrelaxed modulus, relaxed modulus and relaxation time respectively.

In the case of single relaxation, relaxation time is

$$\tau = \tau_0 \exp\left(\frac{\Delta H}{RT}\right) \quad (2)$$

where ΔH is activation energy.

$$\tan\delta(T) = (G_u - G_r)\frac{\omega\tau_0 \exp\left(\frac{\Delta H}{RT}\right)}{G_r + \omega^2\tau_0^2 G_u \exp\left(\frac{\Delta H}{RT}\right)} \quad (3)$$

Integrating this equation gives

$$\int \tan\delta(T)\, d\left(\frac{1}{T}\right) = \frac{(G_u - G_r)}{\sqrt{G_u G_r}} \int_0^\infty \frac{\omega\tau_0 \sqrt{\frac{G_u}{G_r}} \exp\left(\frac{\Delta H}{RT}\right)}{1 + \omega^2\tau_0^2 \left(\sqrt{\frac{G_u}{G_r}}\right)^2 \exp\left(\frac{2\Delta H}{RT}\right)} d\left(\frac{1}{T}\right)$$

$$= \frac{(G_u - G_r)}{\sqrt{G_u G_r}} \frac{R}{\Delta H}\left(\frac{\pi}{2} - \tan^{-1}\omega\tau_0\sqrt{\frac{G_u}{G_r}}\right) \quad (4)$$

Generally, τ_0 is smaller than 10^{-11}, comparing to $\pi/2$, $\tan^{-1}\omega\tau_0\sqrt{G_u/G_r}$ can be omitted.

Thus

$$\frac{2\Delta H}{\pi R}\int \tan\delta(T)\, d\left(\frac{1}{T}\right) = \frac{(G_u - G_r)}{\sqrt{G_u G_r}} = \sqrt{\frac{G_u}{G_r}} - \sqrt{\frac{G_r}{G_u}} \quad (5)$$

The solid lines are fitted curves by using Origin 7 program in Figure 7. The area of $\tan\delta$ is calculated from fitted curves and its values are shown in Table II. As the clay content increases the peak area of $\tan\delta$ is decreased. In Eq. (5) there are two possible cases if the peak area of $\tan\delta$ decreases. Namely, the value of G_u decrease or the value of G_r increase. It represents that the difference between unrelaxed modulus and relaxed modulus is decreased. It means that the nanocomposites show more solid like behavior as the clay content increases.

Nanocomposite materials usually show solidlike or long time relaxation fluid behavior. The prior deformation history of the nanocomposite should be controlled carefully.

The effect of clay loading on linear viscoelasticity of P(MMA-*co*-AN)/clay nanocomposites was investigated. The clay concentration was varied from 5.0 to 10.0 wt%. The nanocomposites show a monotonic increase in storage modulus at all frequencies with increasing silicate content, higher storage moduli than neat copolymer (Figure 8(a)). The effect of clay on storage modulus is very significant, particularly at low frequencies due to the molecular relaxation processes. All nanocomposites exhibit apparent low-frequency plateaus in the linear viscoelastic moduli. This behavior is similar to the response of a viscoelastic solid or a viscoelastic fluid with long characteristic relaxation time. The nanocomposites show a large increase in the complex viscosity with the clay content in Figure 8(b). At high clay loadings, significant shear thinning behavior is observed. They may have yield stress.

The mechanical properties of A0.6M20N20T nanocom-

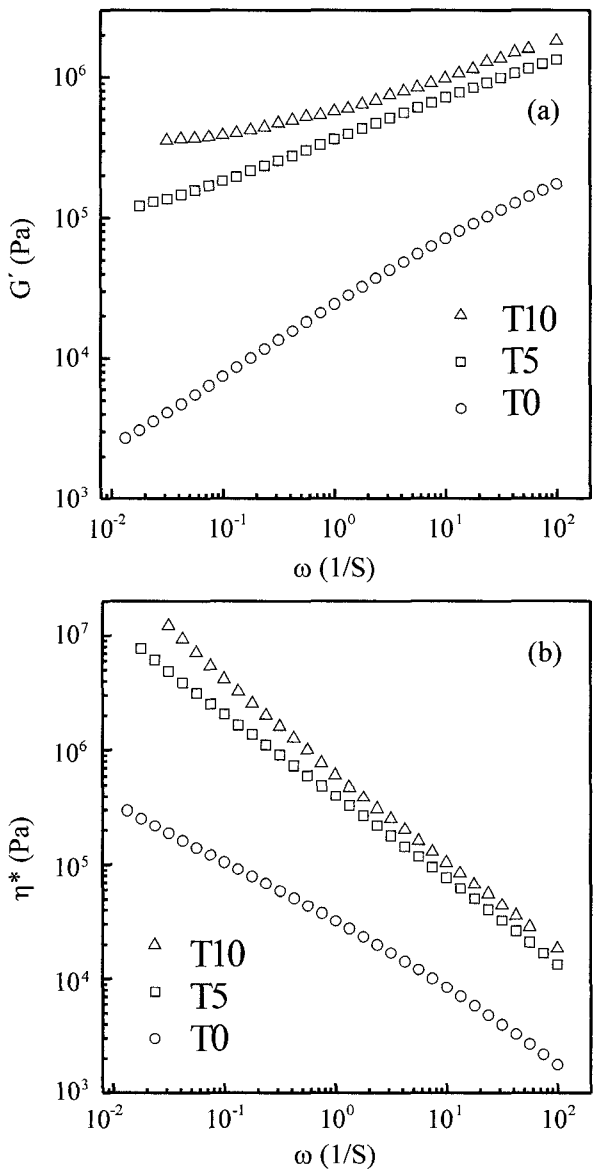

Figure 8. (a) Storage modulus and (b) complex viscosity of A0.6M20N20T nanocomposite series and neat copolymer as a function of frequency at 200 °C.

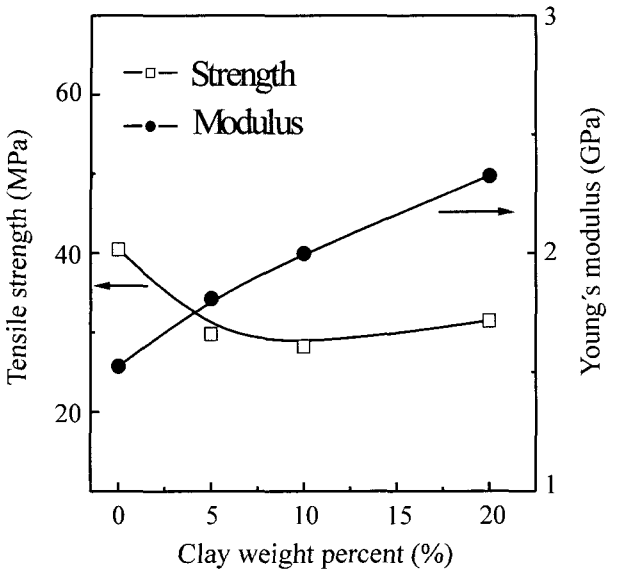

Figure 9. Mechanical property of A0.6M20N20T nanocomposite series and A0.6M20N20T0 neat copolymer as a function of silicate content.

posite series and neat P(MMA-*co*-AN) are shown in Figure 9 as a function of silicate content. Mechanical properties at 0 wt% indicate the mechanical properties of neat P(MMA-*co*-AN). Nanocomposites are larger Young's moduli than neat copolymer. Young's modulus increases steadily as the silicate content increases. At 20 wt% of clay content, A0.6M20N20T20 has Young's modulus of 1.5 times higher than neat P(MMA-*co*-AN). Usually tensile modulus of polymer/clay nanocomposites is related to the morphology of nanocomposites. At low clay contents the modulus increases but at high clay contents the modulus seems to level off. This threshold is consistent with the transition from exfoliated structure to partially exfoliated-partially intercalated structure.[29] In our system modulus shows a constant increment up to 20 wt% due to exfoliated structure of nanocomposites at high clay contents. The strength of nanocomposite is decreased relative to neat P(MMA-*co*-AN) and keep comparable value as the silicate content increases.

Conclusions

A method was described for synthesis of P(MMA-*co*-AN) /Na-MMT nanocomposites through an emulsion polymerization with reactive surfactant AMPS using pristine Na-MMT. The synthesis was carried out by mixing 2-acrylamido-2-methyl-1-propanesulfonic acid (AMPS), comonomer with pristine Na-MMT dispersed in water and then by adding comonomer subsequently. The exfoliated structure of an extracted nanocomposite was further confirmed by TEM.

From XRD patterns of clay dispersions, AMPS widens clay layers and accelerates the insertion of comonomers into clay. The onset temperature of thermal decomposition of A0.6M20N20T20 shifts toward 13.7 °C higher temperature than that of neat copolymer at 20 wt% loss. The dynamic moduli of nanocomposites increase with increasing clay loading. The nanocomposite with 20 wt% of clay shows up to 163% increment in storage modulus relative to neat copolymer. The areas of tanδ of nanocomposites gradually decrease as the clay content of nanocomposites increases. By calculating areas of tanδ of nanocomposites, we observed the nanocomposites show more solid like behavior as the clay content increases. Dynamic storage modulus and complex viscosity increase as the clay content increases. Complex viscosity shows shear-thinning behavior as the clay content increases.

Young's moduli of nanocomposite are higher than that of neat copolymer. Young's moduli increase steadily as the silicate content increases due to the exfoliated structure at high clay contents.

Acknowledgements. Authors would like appreciate financial support from KOSEF (Korea Science and Engineering Foundation) and CAFPoly (Center for Advanced Functional Polymers). This work was also partially supported by the Brain Korea 21 program.

References

(1) T. Lan and T. J. Pinnavais, *Chem. Mater.*, **6**, 2216 (1994).
(2) P. Messersmith and E. P. Giannelis, *Chem. Mater.*, **6**, 1719 (1994).
(3) K. Yano, A. Usuki, A. Okada, T. Kurauchi, and O. Kamigaito, *J. Polym. Sci., Polym. Chem.*, **31**, 2493 (1993).
(4) A. Usuki, M. Kawasumi, Y. Kojima, A. Okada, T. Kurauchi, and O. Kamigaito, *J. Mater. Res.*, **8**, 1174 (1993).
(5) D. C. Lee and L. W. Jang, *J. Appl. Polym. Sci.*, **61**, 1117 (1996).
(6) X. Huang and W. J. Brittain, *Macromolecules*, **34**, 3255 (2001).
(7) X. Fu and S. Qutubuddin, *Mater. Lett.*, **42**, 12 (2000).
(8) X. Huang, S. Lewis, and W. J. Brittain, *Macromolecules*, **33**, 2000 (2000).
(9) J. S. Bergman, H. Chen, E. P. Giannelis, M. G. Thomas, and G. W. Coates, *Chem. Commun.*, 2179 (1999).
(10) K. H. Wang, M. Xu, Y. S. Choi, and I. J. Chung, *Polymer Bulletin*, **46**, 499 (2001).
(11) K. H. Wang, M. H. Choi, C. M. Koo, M. Xu, I. J. Chung, M. C. Jang, S. W. Choi, and H. H. Song, *J. Polym. Sci., Part B: Polym. Phys.*, **40**, 1454 (2002).
(12) J. M. Garces, D. J. Moll, J. Bicerano, R. Fibiger, and D. G. McLeod, *Adv. Mater.*, **12**, 1835 (2000).
(13) G. Galgali, C. Ramesh, and A. Lele, *Macromolecules*, **34**, 852 (2001).
(14) M. J. Solomon, A. S. Almusallam, K. F. Seefeldt, A. Somwangthanaroj, and P. Varadan, *Macromolecules*, **34**, 1864 (2001).
(15) Z. Wang and T. J. Pinnavaia, *Chem. Mater.*, **10**, 3769 (1998).

(16) H. Ishida, S. Campbell, and J. Backwell, *Chem. Mater.*, **12**, 1260 (2000).
(17) J. M. Brown, D. Curliss, and R. A. Vaia, *Chem. Mater.*, **12**, 3376 (2000).
(18) H. L. Tyan, C. M. Leu, and K. H. Wei, *Chem. Mater.*, **13**, 222 (2001).
(19) M. H. Choi, I. J. Chung, and J. D. Lee, *Chem. Mater.*, **12**, 2977 (2000).
(20) J. G. Ryu, J. W. Lee, and H. Kim. *Macromol. Res.*, **10**(4), 187 (2002)
(21) N. Sukpirom and M. M. Lerner, *Chem. Mater.*, **13**, 2179 (2001).
(22) H. Y. Byun, M. H. Choi, and I. J. Chung, *Chem. Mater.*, **13**, 4221 (2001).
(23) L. Liang, J. Liu, and X. Gong, *Langmir*, **16**, 9895 (2000).
(24) Y. S. Choi, M. H. Choi, K. H. Wang, S. O. Kim, Y. K. Kim, and I. J. Chung, *Macromolecules*, **34**, 8978 (2001).
(25) Y. S. Choi, K. H. Wang, M. Xu, and I. J. Chung, *Chem. Mater.*, **14**, 2936 (2002).
(26) M. Seki, Y. Morishima, and M. Kamachi, *Macromolecules*, **25**, 6540 (1992).
(27) P. B. Messersmith and E. P. Giannelis *J. Polym. Sci., Polym. Chem.*, **33**, 1047 (1995).
(28) I. M. Ward, *Mechanical Properties of Solid Polymers*, 2nd ed., Wiley-Interscience, New York, 1983.
(29) M. Alexandre and P. Dubois, *Mater. Sci. Eng.*, **28**, 1 (2000).